Filomat 39:30 (2025), 10791–10797
https://doi.org/10.2298/FIL2530791A

Published by Faculty of Sciences and Mathematics,
University of Niš, Serbia
Available at: http://www.pmf.ni.ac.rs/filomat

# The impact of initial flow velocity and fluid flow direction on the dispersion of quasi-Scholte waves propagating in an orthotropic plate in contact with the fluid

**Reyhan Akbarli**[a]

[a] *Azerbaijan University of Architecture and Construction, Baku, Azerbaijan*

**Abstract.** This work investigates how the initial flow velocity and the direction of the fluid flow influence the dispersion of quasi- Scholte waves traveling through an orthotropic plate in contact with the fluid. The plate's motion is modeled using the exact elastodynamic equations for anisotropic materials, while the fluid's behavior is described by the linearized Euler equations.

## 1. Introduction

This paper explores the influence of the flow velocity and direction of a barotropic, compressible, inviscid fluid in its initial state on the dispersion of quasi-Scholte waves in a hydro-elastic system consisting of an orthotropic plate and the fluid. A thorough review of relevant research is presented in [1, 2, 3, 4, 5, 6] and other cited works. From this review, it becomes clear that previous studies have generally assumed the fluid to be at rest initially, i.e., before wave propagation in the plate-fluid system [7, 8]. Additionally, these studies typically focused on isotropic materials for the plate [9, 10]. In this context, the present work is one of the first to address these factors. Notably, the plate's motion is governed by the exact elastodynamic equations for anisotropic bodies [11], while the fluid flow is described by the linearized Euler equations [12].

Wave propagation in fluid-structure interaction systems has been widely studied due to its significance in various engineering applications, including underwater acoustics, structural health monitoring, and geophysics [13, 14]. Among these, quasi-Scholte waves, which propagate along the interface between a solid and a fluid, have drawn considerable attention due to their unique characteristics and sensitivity to material and environmental conditions [5, 15]. These waves are particularly useful in non-destructive testing and underwater communication technologies, where understanding their behavior can lead to improved system performance [16, 17].

In previous research, wave propagation in fluid-structure systems was typically analyzed under the assumption that the fluid was initially at rest [7, 8]. This simplification allows for easier mathematical modeling but does not account for real-world scenarios where fluids often exhibit motion. For example,

2020 *Mathematics Subject Classification*. Primary 74F10.
*Keywords*. Quasi-Scholte waves, orthotropic plate, compressible inviscid fluid, initial-state fluid flow, wave dispersion.
Received: 05 March 2025; Revised: 07 August 2025; Accepted: 19 September 2025
Communicated by Ljubiša D. R. Kočinac
*Email address:* reyhan.akbarli@azmiu.edu.az (Reyhan Akbarli)
ORCID iD: https://orcid.org/0000-0002-4947-232X (Reyhan Akbarli)

in ocean engineering, pipeline flow systems, and river hydraulics, the presence of moving fluids can significantly alter wave behavior [18]. Additionally, most earlier studies assumed that the solid structure in these systems was isotropic, meaning that its mechanical properties were uniform in all directions [9, 10]. However, many engineering materials, such as composites and layered structures, are orthotropic, meaning they exhibit different mechanical properties along different axes [1, 19].

This study addresses these limitations by investigating the influence of initial fluid velocity and flow direction on quasi-Scholte wave dispersion in a hydroelastic system consisting of an orthotropic plate in contact with a moving fluid. The mathematical formulation incorporates exact elastodynamic equations for anisotropic solids [11] and linearized Euler equations for compressible, inviscid fluids [12]. By including fluid motion as a key parameter, this work aims to provide a more comprehensive understanding of wave behavior in realistic fluid-structure interaction scenarios.

By solving the governing equations and analyzing the resulting dispersion relations, this study reveals how fluid flow affects wave propagation characteristics. The numerical results presented in this paper highlight the significant role that initial flow conditions play in determining the speed and behavior of quasi-Scholte waves [4, 20]. These findings contribute to both theoretical advancements and practical applications in fields such as hydroelasticity, wave mechanics, and material science.

## 2. Problem formulation and solution method

Consider the hydro-elastic system composed of an orthotropic plate, a compressible, barotropic, inviscid fluid, and a rigid wall that restricts the fluid flow. The Cartesian coordinate system $Ox_1x_2x_3$ is associated with the center plane of the plate, and it is assumed that the plate undergoes a plane strain state, while the fluid flow occurs in the $Ox_1x_2$ plane. In the initial state, prior to wave propagation, the fluid flows with a constant velocity $V_0$ along the$Ox_1$axis. A schematic representation of the hydro-elastic system under consideration is shown in Fig. 1. According to this sketch, the regions$\{-\infty < x_1 < +\infty\ ;-h \le x_2 \le +h; -\infty < x_3 < +\infty\}$ and $\{-\infty < x_1 < +\infty\ ;-(h+h_d) \le x_2 \le -h; -\infty < x_3 < +\infty\}$, which are occupied by the plate and the fluid, respectively, can be identified, where$2h$ represents the plate thickness and $h_d$ is the fluid depth.

Based on these assumptions, we aim to study the dispersion of waves propagating along the $Ox_1$ axis within this system. To achieve this, we proceed by formulating the field equations and relationships governing the motion of the plate and the flow of the fluid.

The equation of motion for the plate:

$$\frac{\partial \sigma_{11}}{\partial x_1} + \frac{\partial \sigma_{12}}{\partial x_2} = \rho_P \frac{\partial^2 u_1}{\partial t^2}, \frac{\partial \sigma_{12}}{\partial x_1} + \frac{\partial \sigma_{22}}{\partial x_2} = \rho_P \frac{\partial^2 u_2}{\partial t^2}. \tag{1}$$

The elasticity relations:

$$\sigma_{11} = A_{11}\varepsilon_{11} + A_{12}\varepsilon_{22}, \sigma_{22} = A_{12}\varepsilon_{11} + A_{22}\varepsilon_{22}, \sigma_{12} = 2G_{12}\varepsilon_{12},$$

$$A_{11} = \frac{a_{22}}{a_{11}a_{22} - a_{12}^2}, A_{12} = \frac{a_{12}}{a_{11}a_{22} - a_{12}^2}, A_{22} = \frac{a_{11}}{a_{11}a_{22} - a_{12}^2}, a_{11} = \frac{1 - \nu_{13}\nu_{31}}{E_1},$$

$$a_{12} = -\frac{\nu_{12} + \nu_{13}\nu_{32}}{E_1}, a_{22} = \frac{1 - \nu_{23}\nu_{32}}{E_1}, \nu_{13}E_1 = \nu_{31}E_3,$$

$$\nu_{21}E_2 = \nu_{12}E_1, \nu_{32}E_3 = \nu_{23}E_2,$$

$$\varepsilon_{11} = \frac{\partial u_1}{\partial x_1}, \varepsilon_{22} = \frac{\partial u_2}{\partial x_2}, \varepsilon_{12} = \frac{1}{2}\left(\frac{\partial u_1}{\partial x_2} + \frac{\partial u_2}{\partial x_1}\right). \tag{2}$$

In equations (1) and (2), the standard notation is primarily used. However, the notation in equation (3) is defined as follows: $E_1$, $E_2$, and $E_3$ denote the elastic moduli of the plate material along the $Ox_1$, $Ox_2$, and $Ox_3$axes, respectively. $G_{12}$ represents the shear modulus within the $Ox_1x_2$ plane, $\nu_{ij}$ $(i; j = 1, 2, 3)$ refers to the Poisson's ratio that describes the lateral contraction (expansion) of the material fibers in the $Ox_i$ direction

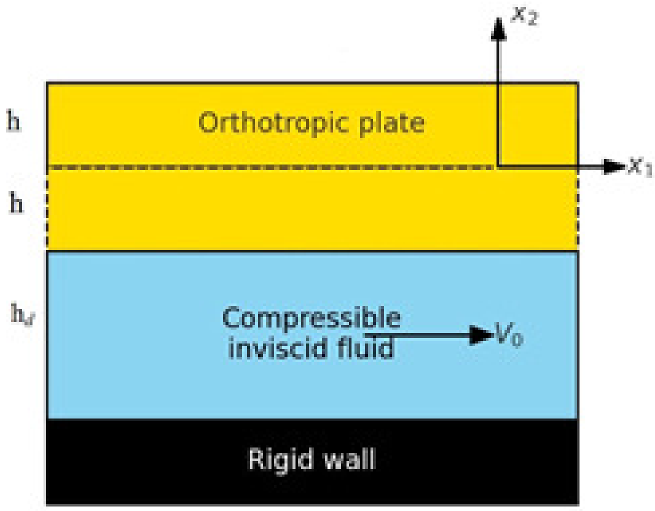


Figure 1: Sketch of the hydro-elastic system under consideration

when stretched (compressed) along the $Ox_j$ axis. Additionally, the subscript $P$in the density $\rho_P$ indicates that this notation pertains to the plate material.

The fluid flow is described by the following linearized Euler equations, as discussed by Chen et al. [6] and Hayashi and Inoue [7]:

$$\frac{\partial V_1}{\partial t} + V_0 \frac{\partial V_1}{\partial x_1} = -\frac{1}{\rho_{0F}} \frac{\partial p'}{\partial x_1}, \frac{\partial V_2}{\partial t} + V_0 \frac{\partial V_2}{\partial x_1} = -\frac{1}{\rho_{0F}} \frac{\partial p'}{\partial x_2}.a_0^2 = \frac{\partial p'}{\partial \rho'},$$

$$\frac{\partial \rho'}{\partial t} + \rho_{0F} \left( \frac{\partial V_1}{\partial x_1} + \frac{\partial V_2}{\partial x_2} \right) + V_0 \frac{\partial \rho'}{\partial x_1} = 0. \tag{3}$$

In equation (3), the notation is defined as follows: $\rho_{0F}$ represents the fluid density before the perturbation caused by wave propagation, $\rho'$ and $p'$ are the perturbations of fluid density and pressure, respectively, $a_0$ is the speed of sound in the fluid, and $V_1$ and $V_2$ are the components of the fluid flow velocity vector in the directions $Ox_1$ and $Ox_2$, respectively. Additionally, $V_0$ in the equation (3) indicates the fluid flow velocity before wave propagation in the hydroelastic system under consideration. Specifically, this work examines the influence of this velocity on the dispersion of propagating waves, a phenomenon also studied in the context of guided wave propagation in fluid-loaded plates [14], [15].

This completes the field equations, and we assume that the following boundary, compatibility, and impermeability conditions are satisfied for the problem under consideration.

$$\sigma_{12}|_{x_2=h} = 0, \ \sigma_{22}|_{x_2=h} = 0, \ \sigma_{12}|_{x_2=-h} = 0, \ \sigma_{22}|_{x_2=-h} = T_{22}|_{x_2=-h},$$

$$\left.\frac{\partial u_2}{\partial t}\right|_{x_2=-h} = v_2|_{x_2=-h}, \ v_2|_{x_2=-h-h_d} = 0. \tag{4}$$

For the solution, all the values sought are expressed as$g(x_1, x_2, t) = \bar{g}(x_2)e^{i(kx_1-\omega t)}$. Substituting this form into the above field equations results in a complete system of ordinary differential equations for these amplitudes. Following this formulation, we examine certain components to determine the amplitudes of the values sought in relation to the plate.

The components of the displacement vector are represented as follows:

$$u_1 = \varphi_1(x_2)\cos(kx_1 - \omega t), u_2 = \varphi_2(x_2)\sin(kx_1 - \omega t). \tag{5}$$

Using the expressions from (2), we derive the following equations for the functions (amplitudes) $\varphi_1(x_2)$and $\varphi_2(x_2)$ in (5) from the equations in (1).

$$\left(\frac{c^2}{c_2^2} - \bar{A}_{11}\right)\varphi_1 + \frac{d^2\varphi_1}{d(kx_2)^2} + (\bar{A}_{12} + 1)\frac{d\varphi_2}{d(kx_2)} = 0,$$

$$\left(\frac{c^2}{c_2^2} - 1\right)\varphi_2 - (1 + \bar{A}_{12})\frac{d\varphi_1}{d(kx_2)} + \bar{A}_{22}\frac{d^2\varphi_2}{d(kx_2)^2} = 0. \tag{6}$$

where

$$c = \frac{\omega}{k}, c_2 = \sqrt{G_{12}/\rho_P}, \bar{A}_{ij} = A_{ij}/G_{12}. \tag{7}$$

By applying the standard solution method to the equations in (6), we obtain the following expressions for the unknown functions $\varphi_1(x_2)$and $\varphi_2(x_2)$.

$$\varphi_2(x_2) = Z_1 e^{\lambda_1 k x_2} + Z_2 e^{-\lambda_1 k x_2} + Z_3 e^{\lambda_2 k x_2} + Z_4 e^{-\lambda_2 k x_2},$$

$$\varphi_1(x_2) = Z_1\delta_1 e^{\lambda_1 k x_2} - Z_2\delta_1 e^{-\lambda_1 k x_2} + Z_3\delta_2 e^{\lambda_2 k x_2} - Z_4\delta_2 e^{-\lambda_2 k x_2}, \tag{8}$$

$$\delta_1 = \frac{c^2/c_2^2 - 1 + \bar{A}_{22}\lambda_1^2}{(\bar{A}_{12} + 1)\lambda_1}, \delta_2 = \frac{c^2/c_2^2 - 1 + \bar{A}_{22}\lambda_2^2}{(\bar{A}_{12} + 1)\lambda_2}, \tag{9}$$

where $\lambda_1$ and $\lambda_2$ in (8) and (9) are the solutions to the characteristic equation given below, an approach that has been explored by various researchers [8], [9].

$$\lambda^4 + L_1\lambda^2 + L_2 = 0, L_1 = \frac{1}{\bar{A}_{22}}\left(\left(\frac{c^2}{c_2^2} - \bar{A}_{11}\right)\bar{A}_{22} + \left(\frac{c^2}{c_2^2} - 1\right) + (\bar{A}_{12} + 1)^2\right),$$

$$L_2 = \frac{1}{\bar{A}_{22}}\left(\frac{c^2}{c_2^2} - \bar{A}_{11}\right)\left(\frac{c^2}{c_2^2} - 1\right). \tag{10}$$

Note that the cases where

$$\left(-\frac{L_1}{2} \pm \sqrt{\frac{L_1^2}{4} - L_2}\right) > 0 \tag{11}$$

we obtain

$$\lambda_1 = \left(-\frac{L_1}{2} + \sqrt{\frac{L_1^2}{4} - L_2}\right)^{\frac{1}{2}}, \lambda_2 = \left(-\frac{L_1}{2} - \sqrt{\frac{L_1^2}{4} - L_2}\right)^{\frac{1}{2}}. \tag{12}$$

However, in the cases where

$$\left(-\frac{L_1}{2} \pm \sqrt{\frac{L_1^2}{4} - L_2}\right) < 0 \tag{13}$$

we derive the following expressions for the functions $\varphi_1(x_2)$and $\varphi_2(x_2)$ :

$$\varphi_2(x_2) = \bar{Z}_1 \cos(\alpha k x_2) + \bar{Z}_2 \sin(\alpha k x_2) + \bar{Z}_3 \cos(\beta k x_2) + \bar{Z}_4 \sin(\beta k x_2),$$

$$\varphi_1(x_2) = \bar{Z}_1 \bar{\delta}_1 \sin(\alpha k x_2) - \bar{Z}_2 \bar{\delta}_1 \cos(\alpha k x_2) + \bar{Z}_3 \bar{\delta}_2 \sin(\beta k x_2) - \bar{Z}_4 \bar{\delta}_2 \cos(\beta k x_2), \tag{14}$$

where

$$\alpha = \left( +\frac{L_1}{2} - \sqrt{\frac{L_1^2}{4} - L_2} \right)^{\frac{1}{2}}, \beta = \left( +\frac{L_1}{2} + \sqrt{\frac{L_1^2}{4} - L_2} \right)^{\frac{1}{2}},$$

$$\bar{\delta}_1 = \frac{c^2 / c_2^2 - 1 - \bar{A}_{22}\alpha^2}{(\bar{A}_{12} + 1)\alpha}, \bar{\delta}_2 = \frac{c^2 / c_2^2 - 1 - \bar{A}_{22}\beta^2}{(\bar{A}_{12} + 1)\beta}. \tag{15}$$

By substituting the expressions from (8) or (14) into the relations in (2), we get the expressions for the amplitudes of the stress tensor components in the plate.

Note that the expressions for the amplitudes of all the sought values involve the unknown constants $Z_1$, $Z_2$, $Z_3$,and $Z_4$ in the case (11), or the unknown constants $\bar{Z}_1$, $\bar{Z}_2$,$\bar{Z}_3$,and $\bar{Z}_4$in the case (13).

Now, consider the procedure for solving the field equations related to fluid flow. To do this, we use the following representation for the fluid flow quantities, based on [3].

$$V_1 = \frac{\partial}{\partial x_1}\Phi_F, V_2 = \frac{\partial}{\partial x_2}\Phi_F, p' = \rho_{0F}\left( V_0 \frac{\partial}{\partial x_1} - \frac{\partial}{\partial t} \right)\Phi_F, \tag{16}$$

where

$$\left[ \Delta - \frac{1}{a_0^2}\left( \frac{\partial}{\partial t} + V_0 \frac{\partial}{\partial x} \right)^2 \right]\Phi_F = 0. \tag{17}$$

Using the presentation

$$\Phi_F = \Phi_{1F}(x_2)\cos(kx_1 - \omega t) \tag{18}$$

and substituting this representation into equation (17), we determine the function$\Phi_{1F}(x_2)$ as follows.

$$\Phi_{1F} = F_1 e^{\chi k x_2} + F_2 e^{-\chi k x_2} if \chi^2 > 0, \tag{19}$$

$$\Phi_{1F} = \bar{F}_1 \cos(\sqrt{-\chi^2} k x_2) + \bar{F}_2 \sin(\sqrt{-\chi^2} k x_2) if \chi^2 < 0, \tag{20}$$

where

$$\chi^2 = 1 - \frac{c^2}{a_0^2} + 2\frac{c}{a_0}\frac{V_0}{a_0} - \frac{V_0^2}{a_0^2}. \tag{21}$$

It is important to note that the constants $F_1$ and $F_2$in (19) (or the constants $\bar{F}_1$ and $\bar{F}_2$in (20)) remain unknown, a detail also addressed by Farhat et al. [11] in the study of wave interactions.

By inserting the expressions from (18)–(21) into the relations in (16), we can then find the amplitudes of the values sought in relation to the fluid.

Once the amplitudes of the sought values are determined and the conditions in (4) are applied, we obtain a system of homogeneous linear algebraic equations for the unknown constants in the amplitude expressions. Setting the determinant of the coefficient matrix of this system equal to zero leads to the corresponding dispersion equation. This equation is solved numerically as part of a numerical investigation , following the procedure described by Bodin et al. [20].

## 3. On the numerical results

In this study, we focus on the dispersion curves derived from the lowest first root of the dispersion equation. These curves pertain to the quasi-Scholte waves in the given problem. An example of these curves, along with the parameters of the problem, is shown in Fig. 2. The analysis of these curves reveals that for the case of $V_0 > 0(V_0 < 0)$, increasing the absolute value of $V_0$ results in either an increase or decrease in the propagation velocity of the quasi-Scholte waves.

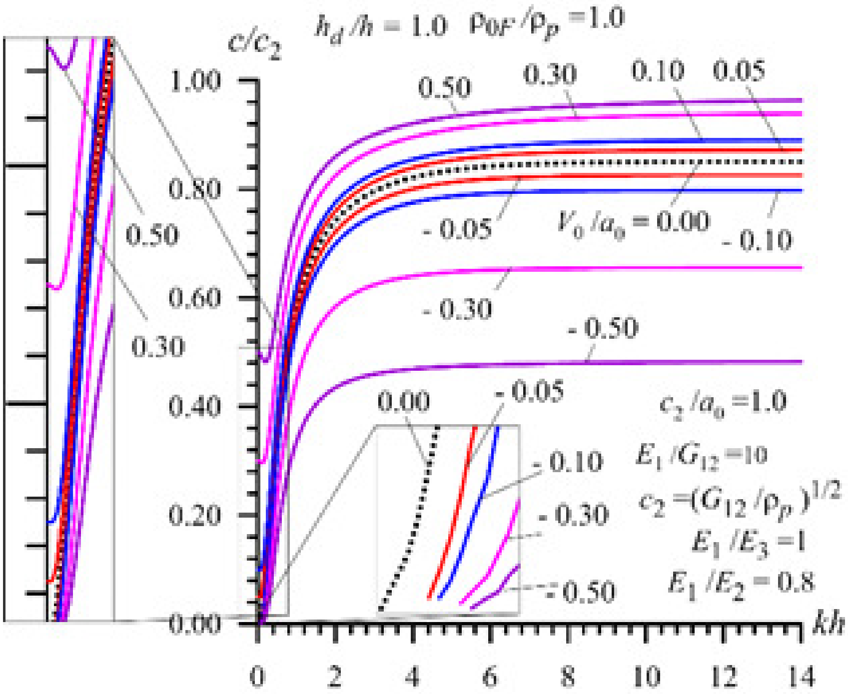


Figure 2: Dispersion curves for the quasi-Scholte waves constructed for various values of the $V_0/a_0$.

From the graphs in Fig. 2, it is evident that when $V_0/a_0 > 0$, the lower wavenumber threshold for the quasi-Scholte wave propagation velocity is greater than zero (it equals zero when $V_0/a_0 = 0$). Moreover, the value of this limiting velocity increases steadily as$V_0/a_0$ increases. This effect highlights how the velocity of the fluid flow affects the propagation speed of the quasi-Scholte waves. Furthermore, for relatively high flow velocities, $V_0/a_0$, a distinct point emerges on the dispersion curve where $d(c/c_2)/d(kh) = 0$. The findings further indicate that increasing $V_0/a_0$ leads to a rise in the propagation speed of the corresponding Scholte waves at the plate-fluid interface.

A closer look at the results in Fig. 2 for the case where $V_0/a_0 < 0$ shows that when the fluid flow opposes the direction of wave propagation, the fluid flow causes the quasi-Scholte wave propagation velocity to decrease. Furthermore, these results demonstrate that for the case $V_0/a_0 < 0$, a cutoff wave number appears, and the values of these wave numbers grow as the absolute value of $V_0/a_0$. When comparing the influence of the fluid flow velocity on the propagation speed of the quasi-Scholte waves, we find that the effect is more significant in the case where $V_0/a_0 < 0$ is larger than in the case where $V_0/a_0 > 0$. At the same time, for $V_0/a_0 < 0$, increasing the absolute value of of $V_0/a_0$ reduces the propagation speed of the corresponding Scholte waves at the plate-fluid interface.

To conclude, we note that the findings presented in Fig. 2 and discussed here are in good qualitative agreement with the results reported in [4], as well as those discussed by Shimpi and Patel [12] and Wu and Mu [18].

## 4. Conclusions

This study demonstrates that when the fluid flow direction aligns with (or opposes) the wave propagation direction, it leads to an increase (or decrease) in the propagation velocity of the quasi-Scholte waves in the plate-fluid system. This conclusion is derived under the assumption that the motion of the plate is governed by the exact linear equations and relations of elastodynamics for orthotropic materials, while the fluid flow is described by the linearized Euler equations for barotropic, compressible, inviscid fluids.

The results obtained are not only of theoretical interest but also have practical implications for potential applications. As a result, the authors plan to continue this research in the future.

## References

[1] S. D. Akbarov, R. S. Akbarli, *Dispersion of quasi-Scholte waves in a hydroelastic system consisting of an orthotropic plate and a compressible fluid layer*, Mechanics of Composite Materials **60** (2025), 1225–1238.

[2] S. D. Akbarov, M. Negin, *Attenuation of quasi-Lamb waves in a hydroelastic system: elastic plate + compressible viscous fluid + rigid wall*, Structural Engineering and Mechanics **81** (2023), 443–459.

[3] A. N. Guz, *Dynamics of Compressible Viscous Fluid*, Cambridge Scientific Publishers, 2009.

[4] S. D. Akbarov, J. N. Imamaliyeva, R. S. Akbarli, *The influence of the fluid flow velocity and direction on the wave dispersion in the initially inhomogeneously stressed hollow cylinder containing this fluid*, Coupled Systems Mechanics **13** (2024), 247–275.

[5] P. Guo, B. Deng, X. Lan, K. Zhang, H. Li, Z. Tian, H. Xu, *Water level sensing in a steel vessel using A0 and Quasi-Scholte waves*, Journal of Sensors 2017 (2017), 1–11.

[6] J. Chen, Z. Su, L. Cheng, *Identification of corrosion damage in submerged structures using fundamental anti-symmetric Lamb waves*, Smart Materials and Structures **19** (2009), 015004.

[7] T. Hayashi, D. Inoue, *Guided wave propagation in metallic and resin plates loaded with water on single surface*, AIP Conference Proceedings **1706**, 030003, 2016. https://doi.org/10.1063/1.4940475

[8] D. Inoue, T. Hayashi, *Transient analysis of leaky Lamb waves with a semi-analytical finite element method*, Ultrasonics **62** (2015), 80–88.

[9] J. Juliá, C. J. Ammon, R. B. Herrmann, A. M. Correig, *Joint inversion of receiver function and surface wave dispersion observations*, Geophysical Journal International **143** (12000), 99–112.

[10] A. M. Bagno, *The dispersion spectrum of a wave process in a system consisting of an ideal fluid layer and a compressible elastic layer*, International Applied Mechanics **51** (2015), 648–653.

[11] M. Farhat, S. Guenneau, S. Enoch, A. B. Movchan, *Cloaking bending waves propagating in thin elastic plates*, Physical Review B **79** (2008), 033102.

[12] R. Shimpi, H. Patel, *A two variable refined plate theory for orthotropic plate analysis*, International Journal of Solids and Structures **43** (2006), 6783–6799.

[13] R. Akbarli, *Features of the behavior of gas-luquid mixture tubes*, International Journal on Technical and Physical Problems of Engineering **12** (2020), 71–77.

[14] Z. Tian, L. Yu, *Study on guided wave propagation in a water loaded plate with wavenumber analysis techniques*, AIP Conference Proceedings 2014.

[15] Z. Tian, L. Yu, *Lamb wave frequency–wavenumber analysis and decomposition*, Journal of Intelligent Material Systems and Structures **25** (2014), 1107–1123.

[16] C. Liao, C. Ma, *Vibration characteristics of rectangular plate in compressible inviscid fluid*, Journal of Sound and Vibration **362** (20151), 228–251.

[17] R. Borsche, R. M. Colombo, M. Garavello, *On the interactions between a solid body and a compressible inviscid fluid*, Interfaces and Free Boundaries Mathematical Analysis Computation and Applications **15** (2013), 381–403.

[18] H. Wu, B. Mu, *On stress concentrations for isotropic/orthotropic plates and cylinders with a circular hole*, Composites Part B Engineering **34** (2003), 127–134.

[19] M. A. Jones, *The separated flow of an inviscid fluid around a moving flat plate*, Journal of Fluid Mechanics **496** (2.0031), 405–441.

[20] T. Bodin, M. Sambridge, H. Tkalcic, P. Arroucau, K. Gallagher, N. Rawlinson, *Transdimensional inversion of receiver functions and surface wave dispersion*, Journal of Geophysical Research Atmospheres **117**(B2) (2011).